

Characterization of masonry under uniaxial tension

Paulo B. Lourenço, Joaquim O. Barros, José C. Almeida

Report 02-DEC/E-12

*The present research has been carried out under
contract GROW-1999-70420 “ISO-BRICK” from the European Commission*

Date: October 2002

No. of pages: 24

Keywords: Tensile Testing, Direct Tension Test, Bricks, Joints.



Escola de
Engenharia



Departamento de
Engenharia Civil



Universidade
do Minho



Contents

1 Introduction	3
2 Materials.....	5
2.1 Bricks	5
2.1.1 HS Bricks	5
2.1.2 HP Bricks	6
2.1.3 S Bricks	6
2.2 Mortar	7
3 Testing Equipment and Applied Measuring Devices.....	8
4 Results and Discussion	9
4.1 Bricks	10
4.1.1 HS Specimens	10
4.1.2 HP Specimens	12
4.1.3 S Specimens	15
4.2 Solid brick-mortar interface specimens	18
5 Conclusions	22
6 References	24

1 Introduction

This report presents the results of a series of masonry and brick specimens under uniaxial tension, aiming at the characterization of Portuguese and Spanish bricks, as well as different typical mortar compositions used in masonry construction.

In a tensile test of a quasi-brittle material, such as brick, it is possible to obtain a stress-elongation diagram $\sigma-u$ in the form indicated in Fig. 1, provided that the test is carried out under displacement control.

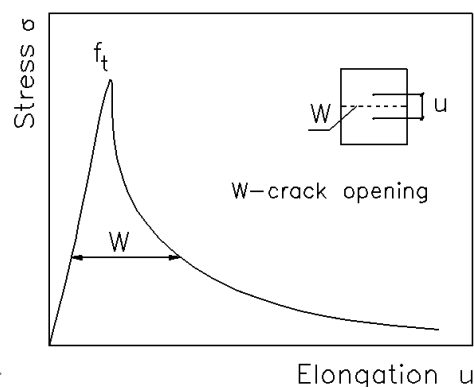


Fig. 1 – Stress-elongation diagram

The illustrated behavior indicates that, after reaching the peak load, the strength does not drop immediately to zero. Instead the strength is gradually reduced in a process denoted as “softening”. The behavior up to peak can be considered linear, but after peak significant non-linearity is found in the response. According to Van Mier (1997), the post-peak behavior can assume two different shapes, as illustrated in Fig. 2, depending on the end restraints of the tested specimen. The behavior in Fig. 2a (rotating platens or hinges) is justified by the rotation of the specimen during the loading operation, where the crack proceeds from one side of the specimen to the other side. In case of Fig. 2b, fixed (non-rotating) platens, a bending moment is introduced and multiple cracks will appear. This results in a slightly larger tensile strength and a higher value of energy dissipated (fracture energy) for materials tested using fixed platens equipment.

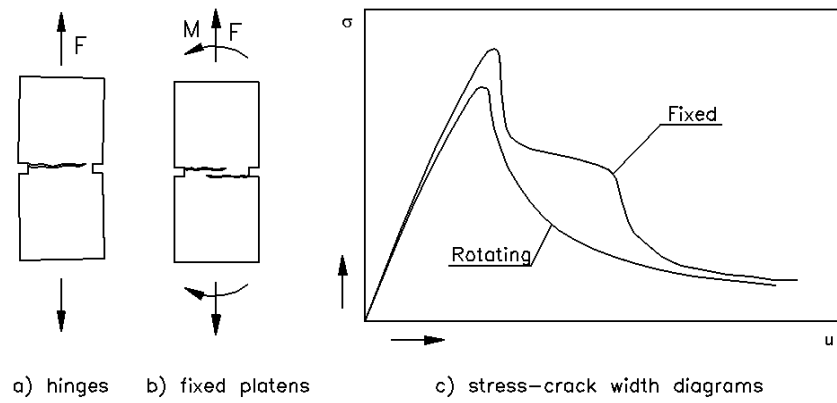


Fig. 2 – Rotating vs. fixed end restraints

2 Materials

2.1 Bricks

Tensile tests were performed with solid (S) bricks, hollow bricks produced in Portugal (HP), and hollow bricks produced in Spain (HS). Each clay brick was tested in vertical (V) and in horizontal (H) direction resulting in six series with the following notation: SV, SH; HPV, HPH; HSV, HSH. Table 1 gives the dimensions of the brick specimens and the free water absorption measured.

Table 1. Series of brick specimens

Bricks	Dimensions [mm]	Free water absorption [mass-%]
S	220 × 110 × 70	9.7
HP	220 × 110 × 70	10.6
HS	240 × 100 × 50	14.6

Notched specimens are required to perform uniaxial tensile deformation controlled tests in homogenous materials. In an attempt to ensure stable tests, the notch where the controller displacement was applied had a depth higher than the notch at the opposite side. The ratio between the depths of these two notches was not kept constant, but the area of the real crack surface (between notches) was measured to evaluate the stress applied. Both notches had 3 mm width.

Grooves were introduced on the brick end surfaces to increase the bond of the specimen to the machine platens.

2.1.1 HS Bricks

This brick has four horizontal holes and a rough top surface. Fig. 3 shows the specimens adopted to characterize the shell and web of the brick, respectively, to the left and right of the figure.



Fig. 3 – Specimens for HSH Units

2.1.2 HP Bricks

To increase the bonding of HP brick specimens to the machine loading platens, the brick end surfaces were grooved. Fig. 4 shows the dimensions of the two types of HP specimens extracted from the bricks, being representative of the brick shell and web.

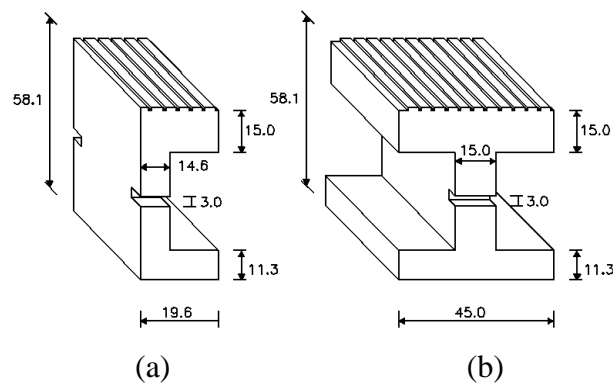


Fig. 4 – HPV Units: Specimens for (a) brick shell and (b) brick web. Dimensions in mm

2.1.3 S Bricks

This type of brick is current on the market and has the dimensions of $220 \times 100 \times 70 \text{ mm}^3$. Due to the maximum load bearing capacity (25 kN), and the space available between the platens of the testing machine (90 mm), $40 \times 40 \times 70 \text{ mm}^3$ S brick specimens were extracted according to the scheme shown in Fig. 5.

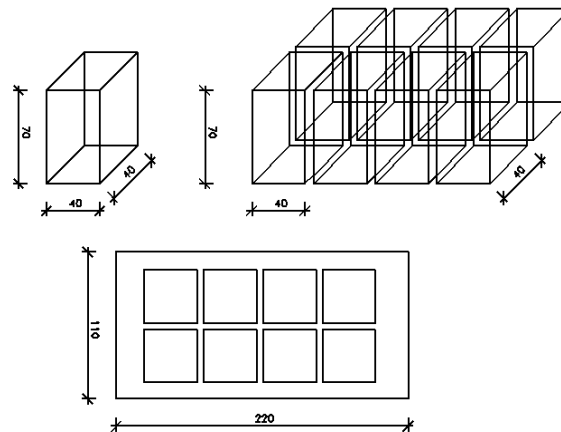


Fig. 3 – SV Units. Dimensions in mm

2.2 Mortar

Four different types of mortars were adopted for the 10 mm thick joint, changing the proportions, in weight, of the (binder):sand, namely: (1):3, (1):4, (1):5 and (1):2:9. In the first three mixes, Portland cement class normal 32.5 was used, featuring a compressive strength of 32.5 N/mm² at 28 days (according to Norm NP EN 196-1, 1990). In the last mix, the binder was made using 1/3 of this cement and 2/3 of hydrated lime. In all mixes, the same natural sand was used, with the following grading (percent of retained material, in weight): sieve #30, 51.3%; sieve #50, 17.0%; sieve #100, 4.5%; sieve #200, 1.8%.

Bending and compression tests were carried out, according to Norm NP EN 196 (1990), to characterize the mortars. The results obtained are given in Table 2.

Table 2. Mortar properties

Mortar	Flexural strength	Compressive strength
	$f_{ct,f}$ (N/mm ²)	f_c (/mm ²)
1:3	4.3	12.8
1:4	3.3	10.9
1:5	1.9	7.1
1:2:9	2.2	6.4

3 Testing Equipment and Applied Measuring Devices

The tensile tests were performed in the laboratory of the Civil Engineering Department of University of Minho, using a CS 7400 – S shearing testing equipment. This machine has two independent hydraulic actuators, positioned in vertical and horizontal directions.

Since three-dimensional non-uniform crack opening can occur on tensile tests, Hordijk (1991), the tensile test control using the average signal of the deformations registered on the four corners of the specimen is the most appropriate procedure, see Fig. 6. However, the available equipment can only control one displacement transducer (LVDT). Therefore, the controller transducer was placed at half height of one saw-cut surface, and another LVDT was positioned on the same place of the opposite surface (see Fig. 7). These transducers have a measurement base of 1 mm with a linearity of 0.17% of the full stroke. A deformation rate of $0.5 \mu\text{m/s}$ was used in the tests. The force applied was measured on a load cell of 25kN maximum load bearing capacity, with an accuracy of 0.03%.

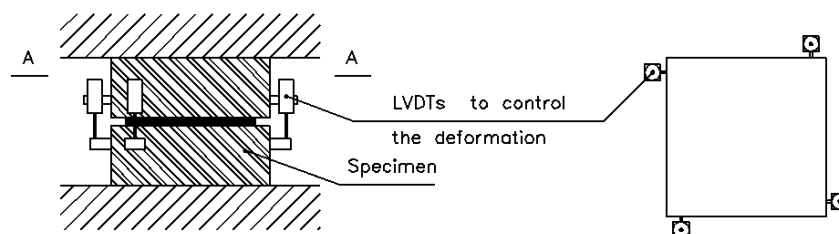


Fig. 6 – Position of LVDTs

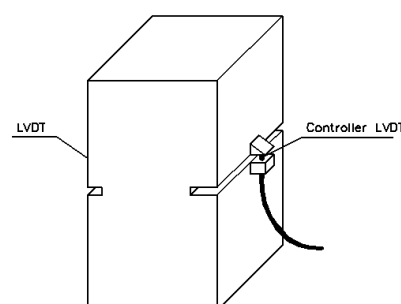


Fig. 7 – Brick specimens

4.1 Bricks

4.1.1 HS Specimens

Figs. 9 and 10 show the stress-elongation relationships recorded on HSV and HSH brick specimens, respectively. Tables 3 and 4 include the values of the main parameters evaluated for these two series of brick specimens. Analyzing the data, it is possible to observe a considerable scatter on the tensile strength, on the fracture energy and on the shape of the softening branch. For the specimens with higher strength, larger stress decay after peak load has occurred. The descending curves of some specimens, sometimes, displayed irregularities, which are due to the non-uniform crack opening, as it was already reported by other researchers, Hordijk (1991).

In the HSV series, 22% of the specimens have failed before attaining the ultimate deformation condition, while in the HSH series this number has increased for 50%. This is most likely due to the orientation of the cracks developed during drying and firing the bricks. In the remainder specimens the test was interrupted for an elongation of 60 μm , when the tensile strength was between 0.2 to 0.5 MPa.

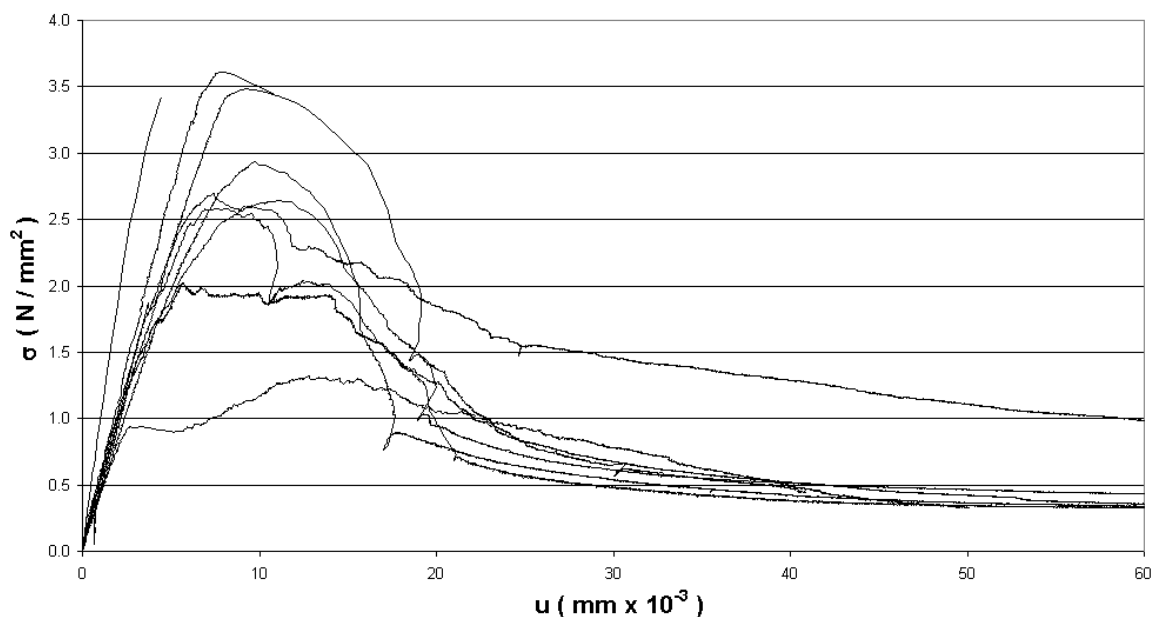


Fig. 9 – Stress-elongation on HSV brick specimens

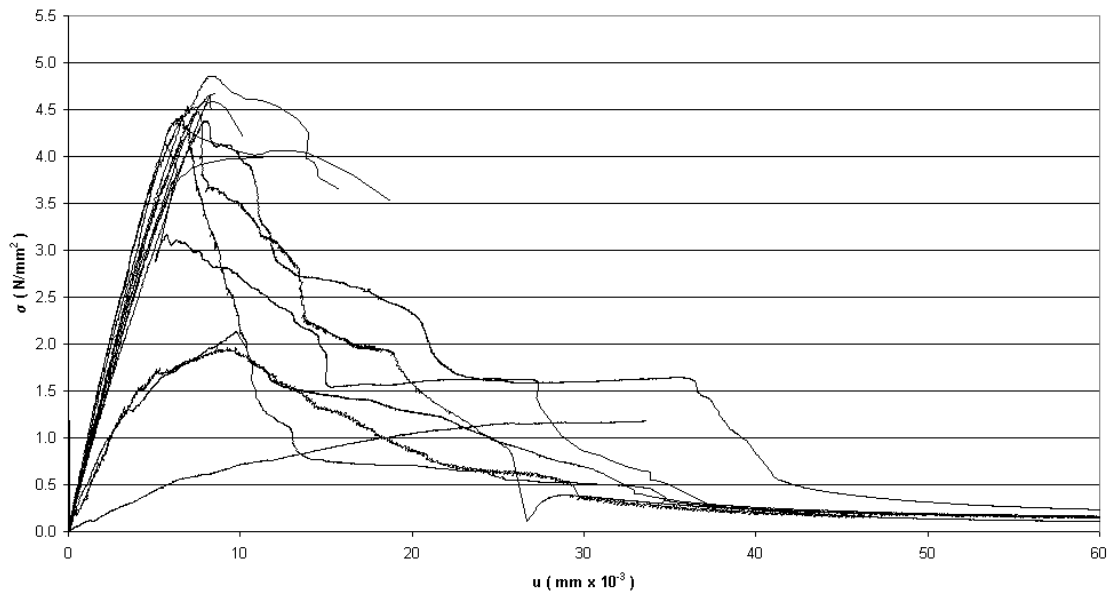


Fig. 10 – Stress-elongation on HSH brick specimens

Table 3. Results on HSV brick specimens

Unit	f_t [N/mm ²]	f_{tu} [N/mm ²]	f_{tu}/f_t [-]	$G_{f,meas}$ [N/mm]
HSV₁	3.43	3.43	100%	-
HSV₃	2.58	0.45	17%	0.04747
HSV₄	2.69	0.69	33%	0.09196
HSV₆	1.32	0.33	25%	0.03629
HSV₇	2.64	0.33	15%	0.05634
HSV₈	3.61	3.45	95%	-
HSV₉	3.48	0.40	15%	0.06948
HSV₁₀	2.93	0.33	15%	0.05275
HSV₁₂	2.02	0.33	16%	0.04681
Mean	2.75			0.05730
CV	27%			32%

Table 4. Results on HSH brick specimens

Unit	f_t [N/mm ²]	f_{tu} [N/mm ²]	f_{tu}/f_t [-]	$G_{fl,meas}$ [N/mm]
HSH₁	4.44	0.16	4%	0.05449
HSH₂	4.58	4.21	92%	-
HSH₂	4.64	4.49	97%	-
HSH₃	2.14	0.11	5%	0.03249
HSH₅	4.13	0.09	2%	0.06507
HSH₆	4.68	4.68	100%	-
HSH₇	3.99	3.99	100%	-
HSH₉	4.86	3.65	75%	-
HSH₁₀	4.38	0.22	5%	0.09347
HSH₁₁	1.18	1.18	100%	-
HSH₁₂	4.26	3.53	83%	-
HSH₁₃	4.48	0.14	3%	0.06297
HSH₁₄	1.97	0.15	8%	0.03402
Mean	3.82			0.05708
CV	32%			40%

Comparing the data obtained in the two series, it was observed that fracture energy is similar in the two directions, but HSH specimens showed a tensile strength 39% higher, due to the extrusion process.

4.1.2 HP Specimens

Figs. 11 and 12 show the stress-elongation relationships obtained on HPV and HPH specimens, respectively. The main data evaluated are included on Tables 5 and 6. Similar to the HS specimens, the tensile strength of HP specimens, loaded horizontally, was higher than the values obtained in the HP specimens loaded vertically (increase of 51%). HPH specimens have developed a fracture energy 53% higher than the one evaluated on HPV specimens.

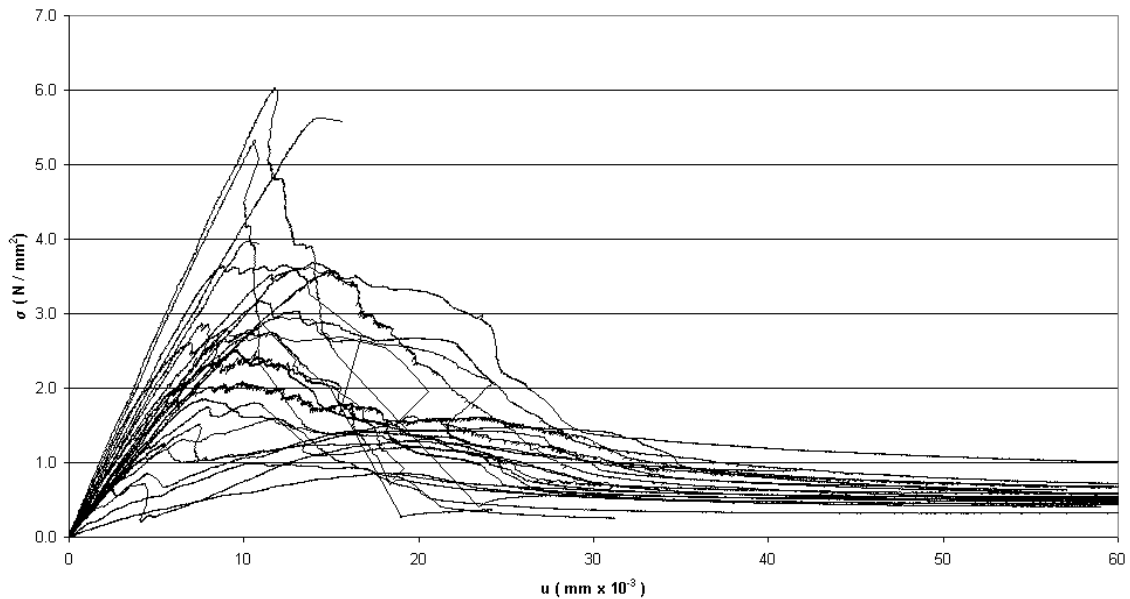


Fig. 11 – Stress-elongation on HPV brick specimens

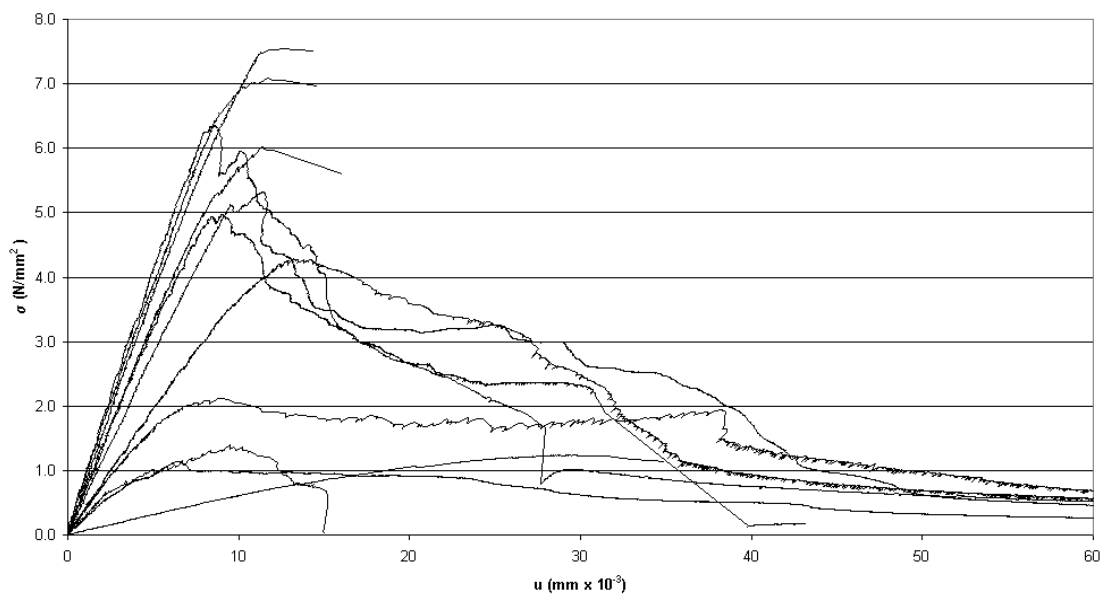


Fig. 12 – Stress-elongation on HPH brick specimens

In HP specimens the scatter of the data registered was significantly higher than the results determined on HS specimens, mainly the tensile strength, which might be related to the manufacturing process (these bricks were manufactured in an old plant, with non-uniform firing temperature). In spite of this, HP specimens have developed tensile strength higher than HS. HPV and HSV have shown similar capacity for dissipating fracture energy, but HPH specimens had higher energy absorption capacity than HSH.

Table 5. Results on HPV brick specimens

Unit	f_t [N/mm ²]	f_{tu} [N/mm ²]	f_{tu}/f_t [-]	$G_{fl,meas}$ [N/mm]
HPV ₁	3.59	0.53	15%	0.06214
HPV ₂	2.65	0.59	22%	0.06334
HPV ₃	3.98	3.93	99%	-
HPV ₄	1.00	0.26	26%	0.01294
HPV ₅	3.17	0.89	28%	0.06741
HPV ₆	3.62	3.36	93%	-
HPV ₇	5.63	5.58	99%	-
HPV ₈	1.85	0.33	18%	0.02553
HPV ₉	2.52	0.52	21%	0.05567
HPV ₁₀	1.28	0.66	52%	0.02305
HPV ₁₁	2.50	0.52	21%	0.05533
HPV ₁₂	1.81	0.42	23%	0.04511
HPV ₁₃	1.49	0.63	43%	0.04671
HPV ₁₄	1.59	0.57	36%	0.05476
HPV ₁₅	2.95	0.53	18%	0.08582
HPV ₁₆	1.52	0.47	31%	0.06064
HPV ₁₇	2.87	0.53	19%	0.06088
HPV ₁₈	1.32	0.47	36%	0.04133
HPV ₁₉	0.86	0.41	48%	0.02721
HPV ₂₀	2.09	0.63	30%	0.06885
HPV ₂₁	2.74	0.59	22%	0.07582
HPV ₂₂	3.60	0.45	13%	0.07586
HPV ₂₃	2.80	0.37	13%	0.02108
HPV ₂₄	6.03	0.45	8%	0.07885
HPV ₂₅	3.69	0.63	17%	0.10657
HPV ₂₆	4.81	4.64	96%	-
HPV ₂₇	5.33	0.48	9%	0.06530
Mean	2.86			0.05566
CV	49%			41%

Table 6. Results on HPH brick specimens

Unit	f_t [N/mm ²]	f_{tu} [N/mm ²]	f_{tu}/f_t [-]	$G_{f, meas}$ [N/mm]
HPH₁	1.14	0.19	16%	0.03722
HPH₂	4.97	0.18	4%	0.09794
HPH₃	2.12	0.42	20%	0.08562
HPH₄	4.28	0.38	9%	0.11637
HPH₅	1.24	1.14	92%	-
HPH₃	6.03	5.61	93%	-
HPH₄	1.41	0.03	2%	0.01217
HPH₅	7.54	7.50	100%	-
HPH₆	7.09	6.97	98%	-
HPH₇	5.32	0.31	6%	0.13136
HPH₈	6.36	0.39	6%	0.11609
Mean	4.32			0.08525
CV	57%			52%

4.1.3 S Specimens

The stress-elongation relationships for specimens SV and SH are depicted on Figs. 13 and 14, respectively. The main data evaluated is included on Tables 7 and 8. The SV series had a tensile strength 18% higher and fracture energy 15% higher than the values obtained on SH series. Like in previous series, the scatter on the S series was also too high, particularly, on the tensile strength of SH series. After testing, internal cracks and voids in some bricks were observed, justifying the obtained scatter. The tensile strength and the fracture energy of S series were of the same order of the HS and HP series.

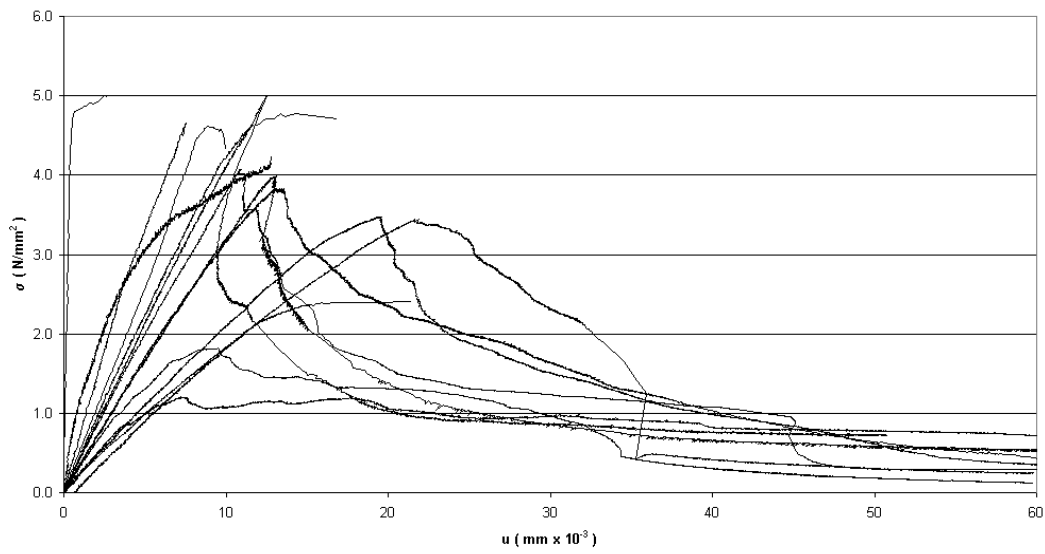


Fig. 13 – Stress-elongation on SV brick specimens

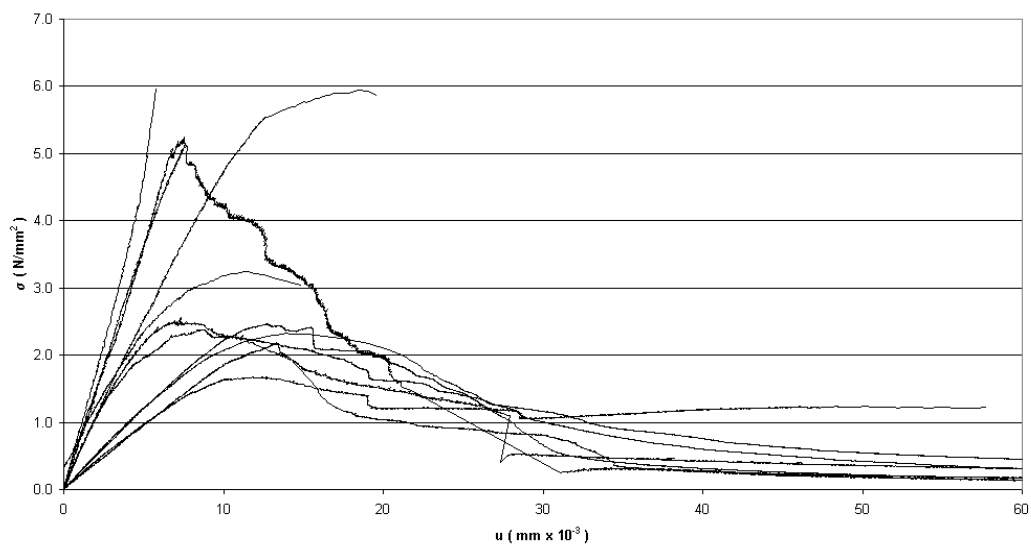


Fig. 14 – Stress-elongation on SH brick specimens

Table 7. Results on SV specimens

Unit	f_t [N/mm ²]	f_{tu} [N/mm ²]	f_{tu}/f_t [-]	$G_{fl, meas}$ [N/mm]
SV₁	1.21	0.20	17%	0.05460
SV₂	3.83	3.70	97%	-
SV₃	3.48	0.19	5%	0.08083
SV₄	3.45	0.25	7%	0.04285
SV₅	0.84	0.51	60%	0.02842
SV₆	0.89	0.16	18%	0.02580
SV₇	1.82	0.12	7%	0.04307
SV₉	5.00	4.99	100%	-
SV₁₀	4.62	4.33	94%	-
SV₁₃	3.83	0.28	7%	0.09179
SV₁₄	4.66	4.48	96%	-
SV₁₇	4.08	0.23	6%	0.07864
SV₁₉	4.23	4.21	99%	-
SV₂₂	5.00	0.72	14%	0.06075
SV₂₃	4.78	4.71	99%	-
SV₂₄	3.99	0.11	3%	0.06861
Mean	3.48			0.05754
CV	42%			39%

Table 8. Results on SH specimens

Units	f_t [N/mm ²]	f_{tu} [N/mm ²]	f_{tu}/f_t [-]	$G_{fl,meas}$ [N/mm]
SH₁	2.47	0.15	6%	0.05227
SH₂	1.68	1.22	73%	0.06045
SH₃	2.32	0.40	17%	0.06638
SH₄	0.69	0.24	35%	-
SH₆	0.80	0.16	21%	0.00954
SH₇	0.81	0.18	22%	0.03051
SH₈	2.18	0.16	7%	0.03961
SH₉	2.56	0.29	11%	0.05784
SH₁₀	5.97	5.97	100%	-
SH₁₃	5.09	5.02	99%	-
SH₁₅	2.38	0.17	7%	0.06029
SH₁₇	5.95	5.87	99%	-
SH₁₈	3.24	3.04	94%	-
SH₁₉	5.25	0.12	2%	0.07656
Mean	2.96			0.05083
CV	63%			41%

4.2 Solid brick-mortar interface specimens

Figs. 15 to 17 illustrate the stress-elongation relationships for specimens composed by two halves of SV bricks connected by the type of mortars described on Section 2.2. The main data evaluated is included on Tables 9 to 11.

These tests were rather unstable and the softening branch could be obtained only in a few tests. The values of the fracture energy and the tensile strength were lower than the values registered on the brick-only specimens. The highest tensile strength was found on specimens with a 1:4 mortar joint.

The results of the specimens with a 1:5 mortar joint are not presented, because their load bearing capacity was negligible.

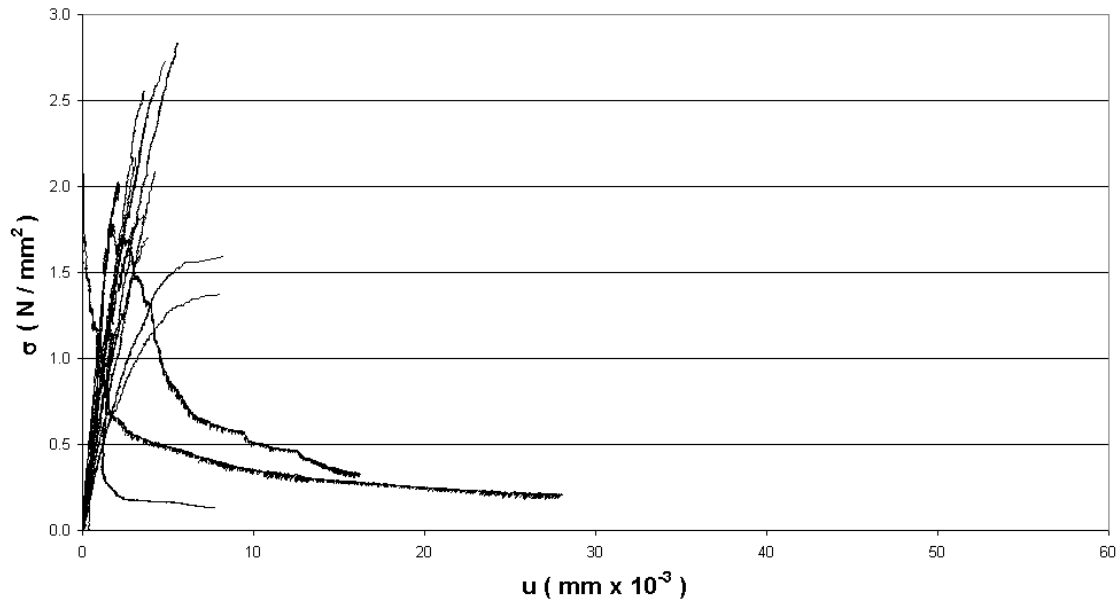


Fig. 15 – Stress-elongation on specimens SV-1:3 mortar

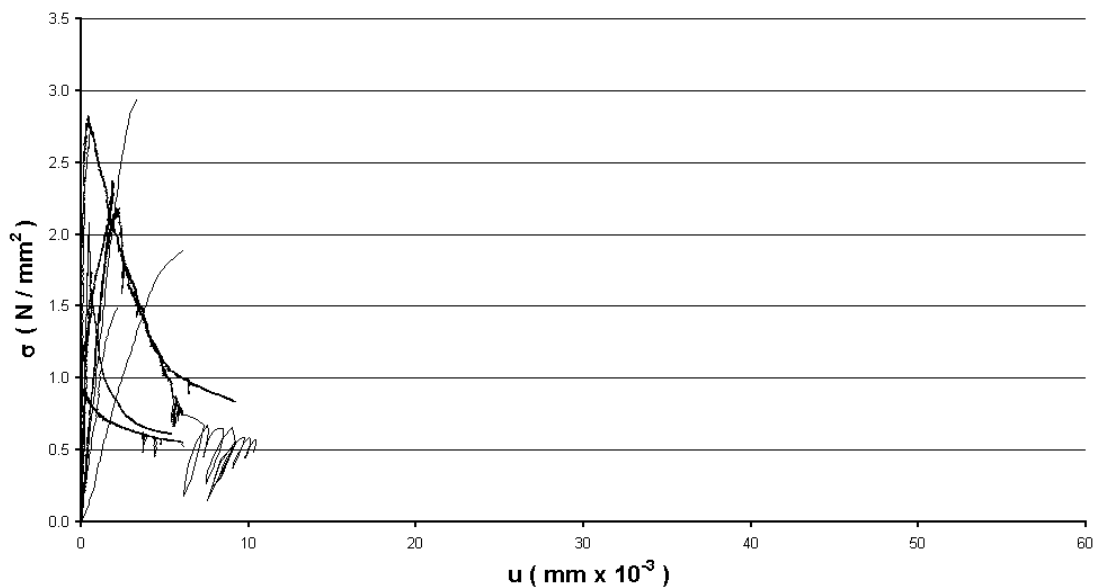


Fig. 16 – Stress-elongation on specimens SV-1:4 mortar.

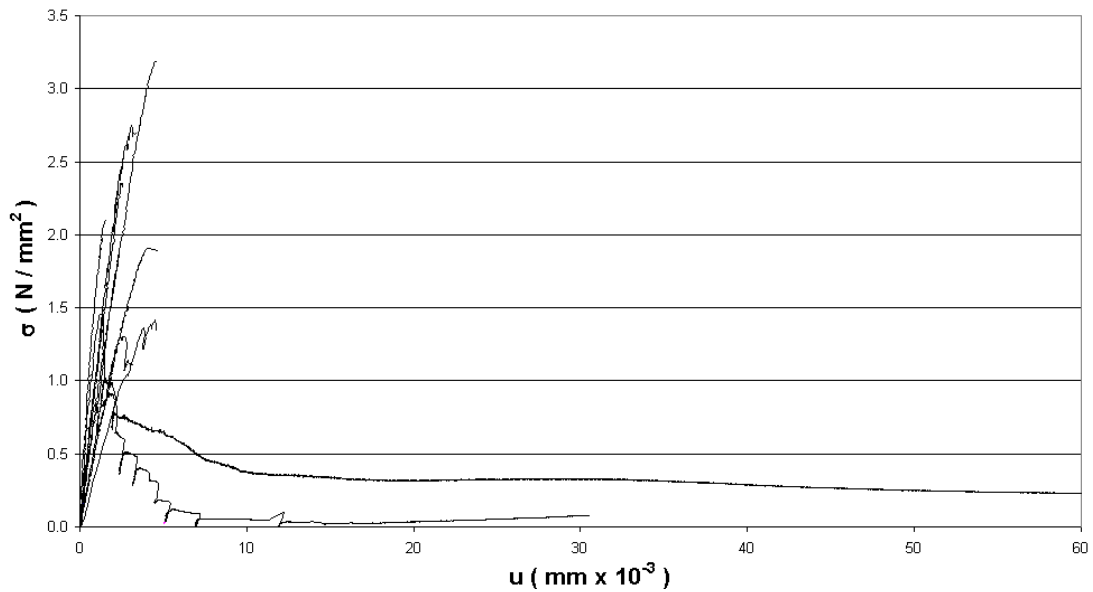


Fig. 17 – Stress-elongation on specimens SV-1:2:9 mortar

Table 9. Results on specimens SV-1:3 mortar

Unit	f_t [N/mm ²]	f_{tu} [N/mm ²]	f_{tu}/f_t [-]	$G_{ft,meas}$ [N/mm]
M₁	2.77	2.77	100%	-
M₂	2.01	2.01	100%	-
M₃	2.17	2.17	100%	-
M₄	1.70	1.70	100%	-
M₇	2.03	2.00	99%	-
M₉	1.15	0.13	12%	0.00167
M₁₀	2.10	0.21	10%	0.01062
M₁₁	1.37	1.37	100%	-
M₁₂	2.56	2.54	99%	-
M₁₃	2.09	2.09	100%	-
M₁₄	2.73	2.73	100%	-
M₁₅	1.78	0.33	18%	0.01209
M₁₆	2.84	2.83	100%	-
M₁₇	1.59	1.59	100%	-
Mean	2.06			0.00813
CV	25%			69%

Table 10. Results on specimens SV-1:4 mortar

Unit	f_t [N/mm ²]	f_{tu} [N/mm ²]	f_{tu}/f_t [-]	$G_{fl,meas}$ [N/mm]
M₁₈	2.82	0.837	30%	0.01290
M₁₉	2.75	2.747	100%	-
M₂₁	1.90	1.896	100%	-
M₂₂	2.94	2.944	100%	-
M₂₇	2.19	0.491	22%	0.01065
M₂₈	2.08	0.609	29%	0.00459
M₃₀	1.50	1.495	100%	-
M₃₁	2.37	0.513	22%	0.00302
M₃₂	1.74	1.739	100%	-
Mean	2.25			0.00779
CV	22%			61%

Table 11. Results on specimens SV-1:2:9 mortar

Unit	f_t [N/mm ²]	f_{tu} [N/mm ²]	f_{tu}/f_t [-]	$G_{fl,meas}$ [N/mm]
M₃₃	2.75	2.70	98%	-
M₃₄	0.91	0.08	9%	0.0234
M₃₅	1.46	0.19	13%	-
M₃₆	2.11	2.11	100%	-
M₃₉	2.35	2.32	99%	-
M₄₀	1.41	1.34	95%	-
M₄₃	1.31	1.10	84%	-
M₄₅	1.89	1.65	87%	-
M₄₆	3.19	3.19	100%	-
M₄₇	1.91	1.89	99%	-
Mean	1.93			-
CV	36%			-

5 Conclusions

The present report aims at characterizing the tensile behavior of hollow bricks produced in Portugal (HP), hollow bricks produced in Spain (HS), solid bricks produced in Portugal (S) and brick-mortar interface. Three different producers have provided the bricks. To accomplish this purpose, tensile tests on a servo-controlled machine were carried out. The results were obtained under controlled displacement, in order to obtain, not only the tensile strength, but also the shape of the softening branch and the energy dissipated up to a very low residual strength (fracture energy).

Two types of specimens were extracted from the hollow bricks, so that the shell and the web can be characterized. All bricks were tested in vertical (V) and horizontal (H) direction. Due to the brittle behavior of clay brick units, in a significant number of specimens it was not possible to evaluate the fracture energy, since the test was interrupted before attained the deformation limit considered reasonable for assuming that the energy dissipated on cracking process was consumed.

Due to the difficulties of assuring material and geometric homogeneity amongst brick specimens, a large scatter on the tensile strength and on the fracture energy was obtained. This scatter is typical of masonry materials under tension, see van der Pluijm (1999).

Brick specimens exhibit very similar results, if one takes into consideration that three different brick manufacturers have been considered. An average value of the tensile strength in the order of 3 N/mm^2 was obtained. In general, higher strength seems to be obtained in the extrusion direction even if S series results are difficult to understand due to the extremely large scatter. The series of brick specimens have developed average fracture energy values between 0.05 and 0.08 N/mm, the lowest average value was registered on SH series and the highest one on HPH series.

Due to the straight bond crack between brick and mortar, the post peak behavior could be tracked only in a very few specimens. In these specimens the average bond tensile strength was in the order of 2 N/mm^2 and the average fracture energy was extremely low (around 0.008 N/mm). It is noted the value of the interface fracture energy is around one tenth of the brick fracture energy. No significant differences were found with respect to the



different mortar mixes (1:3, 1:4 and 1:2:9), with the exception of mortar mix 1:5 that resulted in (too weak) non-measurable bond.

It is noted that the bond strength values obtained in the present paper are higher than in some literature, see e.g. van der Pluijm (1999). The reason for this difference seems to be related to the process of preparing the specimens. Here, the specimens were cast in groups of sixteen, pressed between two moulds so that a mortar thickness of 10 mm was found and, finally, the individual specimens were separated while the mortar was fresh. As a result, the actual bond area obtained in the present testing program was almost the full specimen. On the contrary, in van der Pluijm (1999) the actual bonding area was only 35% of the specimen cross section.



6 References

Hordijk, D.A. Local approach to fatigue of concrete, PhD Thesis, Technical University of Delft, Netherlands, 1991.

NP EN196-1 Methods for testing cement (in Portuguese) (1990).

van der Pluijm, R., Out-of-plane Bending of Masonry Behavior and Strength, PhD Thesis, Eindhoven University of Technology, 1999.

van Mier, Fracture Processes of Concrete, CRC Press, New York, 1997.